

Proximity induced metal/insulator transition in $\text{YBa}_2\text{Cu}_3\text{O}_7/\text{La}_{2/3}\text{Ca}_{1/3}\text{MnO}_3$ superlattices

Todd Holden,^{1,2,*} H-U. Habermeier,¹ G. Cristiani,¹ A. Golnik,^{3,1} A. Boris,¹ A. Pimenov,¹ J. Humlíček,^{4,1} O. Lebedev,⁵ G. Van Tendeloo,⁵ B. Keimer,¹ and C. Bernhard¹

¹*Max-Planck-Institut für Festkörperforschung, Heisenbergstrasse 1, D-70569 Stuttgart, Germany*

²*Physics Department, Brooklyn College of the City University of New York, Brooklyn, New York 11210*

³*Institute of Experimental Physics, Warsaw University, 69 Hoża, 00-681 Warszawa, Poland*

⁴*Department of Solid State Physics, Masaryk University, Kotlářská 2, CZ-61137 Brno, Czech Republic*

⁵*University of Antwerpen, EMAT RUCA, B-2020 Antwerp, Belgium*

(Dated: November 19, 2018)

The far-infrared dielectric response of superlattices (SL) composed of superconducting $\text{YBa}_2\text{Cu}_3\text{O}_7$ (YBCO) and ferromagnetic $\text{La}_{0.67}\text{Ca}_{0.33}\text{MnO}_3$ (LCMO) has been investigated by ellipsometry. A drastic decrease of the free carrier response is observed which involves an unusually large length scale of $d^{\text{crit}} \approx 20$ nm in YBCO and $d^{\text{crit}} \approx 10$ nm in LCMO. A corresponding suppression of metallicity is not observed in SLs where LCMO is replaced by the paramagnetic metal LaNiO_3 . Our data suggest that either a long range charge transfer from the YBCO to the LCMO layers or alternatively a strong coupling of the charge carriers to the different and competitive kind of magnetic correlations in the LCMO and YBCO layers are at the heart of the observed metal/insulator transition. The low free carrier response observed in the far-infrared dielectric response of the magnetic superconductor $\text{RuSr}_2\text{GdCu}_2\text{O}_8$ is possibly related to this effect.

I. INTRODUCTION

The coexistence of such antagonistic phenomena as superconductivity (SC) and ferromagnetism (FM) is a long-standing problem in solid state physics. Originally it was believed that they were mutually exclusive, but more recently it was found that they can coexist under certain circumstances giving rise to novel kinds of combined ground states¹. Renewed interest in SC and FM systems has been spurred by the search for novel materials for applications in spintronic devices² as well as by the observation that for a number of materials (including the cuprate high- T_c 's) superconductivity occurs in the vicinity of a magnetic instability^{3,4}.

Artificially grown heterostructures and superlattices (SLs) of alternating SC and FM materials have become an important tool for exploring the interplay between SC and FM. Of particular interest have been SLs of perovskite-like transition metal oxides which allow one to combine for example the cuprate high T_c superconductor (HTSC) $\text{YBa}_2\text{Cu}_3\text{O}_7$ (YBCO) with $T_c=92$ K with the manganite compound $\text{La}_{2/3}\text{Ca}_{1/3}\text{MnO}_3$ (LCMO) that exhibits colossal magnetoresistance (CMR) and a FM ground state below $T^{\text{Curie}}=240$ K. The similar lattice constants and growth conditions of YBCO and LCMO have enabled several groups to grow SL's using various techniques like molecular beam epitaxy⁵, laser ablation^{6,7}, or magnetron- and ion beam sputtering^{8,9,10,11}. Transport and magnetization measurements on these SL's have established that there is a strong interaction between the SC and FM order parameters in these SLs since both T_c and T_{mag} are considerably suppressed^{6,10}. This suppression is most pronounced for SLs with similarly wide YBCO and LCMO layers. Notably, a sizeable suppression of T_c and T_{mag}

was observed even for SLs with relatively thick layers of $d_{\text{YBCO}}, d_{\text{LCMO}} > 10$ nm. This observation implies that the proximity coupling involves an unexpectedly large length scale far in excess of the SC coherence length of $\xi_{\text{SC}} \leq 2$ nm. Equally remarkable are some reports of a considerable suppression of the normal state electronic conductivity^{8,10,11} which at a first glance is not expected since these SLs are composed of metallic materials.

These puzzling observations motivated us to investigate the electronic properties of SC/FM SLs by means of spectral ellipsometry. Unlike transport measurements, this optical technique is not plagued by contact problems and allows one to reliably obtain the bulk electronic properties of a given material since grain boundaries with lower conductivity or filamentary pathes of least resistance do not contribute significantly. We investigated the far-infrared dielectric properties of a series of SLs that are composed of thin layers of YBCO and LCMO. Our optical data provide clear evidence that the free carrier response in these SC/FM SLs is strongly suppressed as compared to the pure films of which they consist. The suppression appears in the normal state as well as in the SC state. It depends strongly on the thickness ratio, $d_{\text{YBCO}}/d_{\text{LCMO}}$, and is most pronounced for a 1:1 ratio. Our most important observation is that the length scale involved is surprisingly large with nearly complete suppression for layer thicknesses of $d_{\text{YBCO}}^{\text{crit}} \approx 20$ nm and $d_{\text{LCMO}}^{\text{crit}} \approx 10$ nm. A similar suppression is observed for SLs that are composed of YBCO and the FM metal SrRuO_3 (SRO). In stark contrast, we observe no corresponding suppression of metallicity in similar SLs that consist either of YBCO and the paramagnetic metal LaNiO_3 (LNO) or of the insulating compound $\text{PrBa}_2\text{Cu}_3\text{O}_7$ (PBCO).

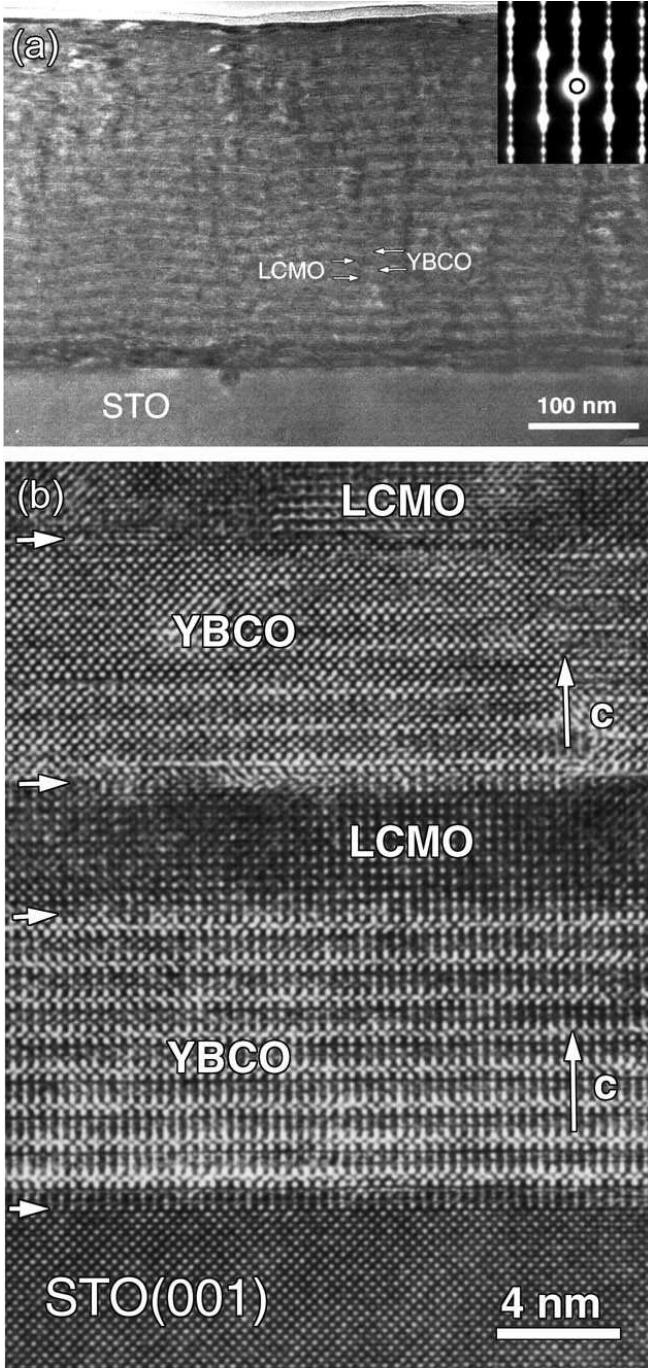


FIG. 1: (a) Low resolution (b) high resolution transmission electron microscope and electron diffraction (shown on inset) images of a $[8\text{nm}:6\text{nm}]\times 20$ superlattice. Note that the first YBCO and LCMO layer thicknesses differ from the others.

II. EXPERIMENTAL DETAILS

We have grown SLs of YBCO/LCMO, YBCO/SRO, YBCO/LNO, YBCO/PBCO and also films of the pure materials by laser ablation on SrTiO_3 substrates as described in Ref. 6. The composition of the films and their

high quality has been confirmed by x-ray diffraction analysis, transmission electron microscopy (TEM) and also by Raman measurements. A TEM image of a $[8:6\text{nm}]\times 20$ YBCO/LCMO SL is displayed in Fig. 1. It shows that the interfaces are atomically sharp and epitaxial. When viewed at low magnification the interfaces appear somewhat wavy. A similar waviness is commonly observed in SLs containing YBCO and most likely is related to strain relaxation¹². The X-ray diffraction patterns exhibit only the corresponding (00h) peaks for YBCO, LCMO, and for the SrTiO_3 substrate confirming the phase purity and the epitaxial growth of the SLs. The SL peaks are not well resolved from the main peaks due to the low resolution of the instrument and the interface waviness. The SC and the FM transition temperatures as determined by measurements of the dc-conductivity and SQUID magnetization are summarized in Table I.

The ellipsometric measurements have been performed with a home-built setup at the U4IR and U10A beamlines of the National Synchrotron Light Source (NSLS) in Brookhaven, USA and, in parts, using the conventional mercury arc lamp of a Bruker 113V FTIR spectrometry^{13,14}. In practice, the pseudo-dielectric function for an anisotropic crystal deviates only slightly from the actual dielectric function along the plane of incidence (ab-plane in our case)^{13,15}. The spectra were analyzed with a multilayer ellipsometric analysis program. The film thickness was refined by minimizing features in the calculated film pseudo-dielectric function that arise from the phonons of the SrTiO_3 substrate. It was generally found to agree well with the nominal thickness based on the growth conditions and the TEM data. In many spectra, small artifacts remain due to the Berreman mode near 480 cm^{-1} and the STO phonons near 170 and 550 cm^{-1} , due to small differences of our substrates from the STO reference^{13,16}. Since the SL thickness is well below the FIR wavelength, the entire SL can be treated as a single layer according to effective medium theory. Accordingly an effective dielectric function can be obtained which, for this geometry, corresponds to the volume average of the dielectric functions of the components of the SL¹⁷. Below we will use ϵ_1 and σ_1 to denote the a SL's effective dielectric function and corresponding effective conductivity when discussing SLs.

III. RESULTS AND DISCUSSION

Figure 2 shows representative spectra for the real-parts of the in-plane conductivity, σ_1 , and the dielectric function, ϵ_1 , of several YBCO/LCMO SLs with a thickness ratio close to 1:1, of (a) 60:60 nm, (b) 16:16 nm, (c) 8:6 nm, and (d) 5:5 nm. Shown are spectra in the normal and in the SC state. Given the metallic properties of the pure YBCO and LCMO films (spectra are not shown) one would expect that the SLs also should exhibit a strong metallic response. Instead Figure 2(a-d) highlights that the YBCO/LCMO SLs exhibit a drastic decrease in the

TABLE I: Physical parameters for representative SLs and Films grown by Laser Ablation

[dYBCO:dLCMO]	T_c (K)	T_{mag} (K)	$\omega_p^2(10K)$ (eV ²)	$\Gamma(10K)$ (eV ²)	$\omega_p^2(100K)$ (meV)	$\Gamma(100K)$ (meV)	$\omega_p^2(300K)$	$\Gamma(300K)$
[8nm:6nm]x20	60	120	0.035	49	0.029	49	0.024	50
[5nm:5nm]x40	60	120	0.026	31	0.025	28	0.025	21
[16nm:16nm]x10	73	215	0.36	26	0.29	33	0.11	32
[60nm:60nm]x5	85	245	0.63	22	0.55	33	0.37	66
[60nm:15nm]x5	86	160	1.44	27	1.41	49	1.14	79
[30nm:15nm]x5	80	165	0.80	27	0.84	43	0.7	65
[13nm:5nm]x20	56	115	0.44	29	0.43	38	0.36	66
[8nm:3nm]x20	60	120	0.55	34	0.55	43	0.46	54
[15nm:30nm]x5	-	195	0.39	44	0.22	44	0.12	38
[15nm:60nm]x5	-	240	1.03	42	0.80	43	0.064	21
[dYBCO:dLNO]								
[5nm:5nm]x20	33	-	1.15	69	1.10	72	1.04	76
[10nm:10nm]x20	70	-	1.19	57	1.21	60	1.07	72
[dYBCO:dPBCO]								
[10nm:10nm]x20	85	-	0.36	12	0.57	31	0.49	48
Pure Materials								
YBCO	90	-	0.93	19	1.22	42	1.03	75
LCMO	-	245	1.08	37	0.61	37	0.03	10
LNO	-	-	0.99	103	0.95	98	1.04	111
Ru-1212	-	145	0.30	28	0.28	32	0.24	53

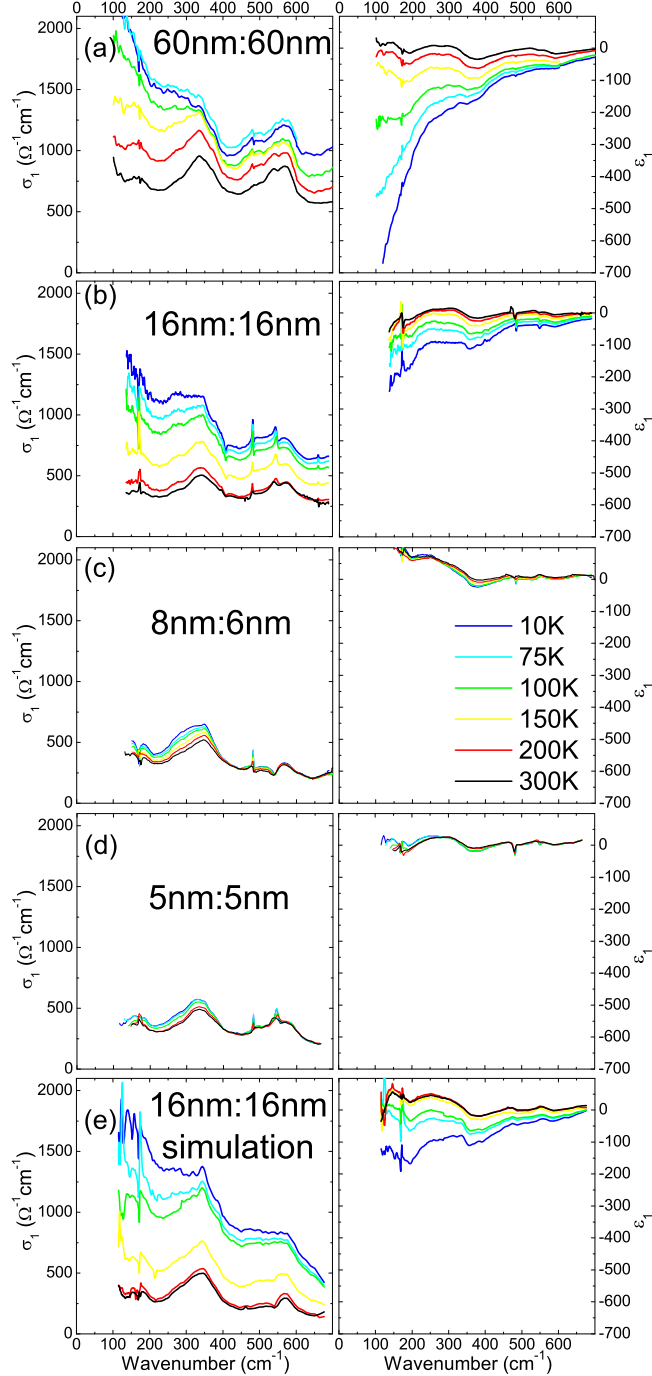
absolute value of σ_1 and ε_1 which corresponds to a significant reduction of the free carrier concentration or of their mobility. This suppression of metallicity is still fairly weak for the 60:60nm SL but becomes sizeable already for the 16:16nm SL. Finally, for the 8:6nm and 5:5nm SLs, the free carrier response is barely visible and the spectra are dominated by phonon modes that are characteristic for LCMO and YBCO. We only note here that we observe a similar effect for the SLs of YBCO/SRO which contain the FM metal SRO.

For a quantitative description of the free carrier response we have modelled the spectra with a Drude-function plus a sum of Lorentzian functions that account for the phonon modes and the so-called MIR-band at higher frequencies. The square of the extracted plasma frequency, $\omega_p^2 = 4\pi n/m^*$, which is proportional to the ratio of the free carrier concentration, n , divided by their effective mass, m^* , are given in table I (at 10K, 100K, and 300 K). The value of ω_p^2 is proportional to the free carrier spectral weight (SW), which is the dominant contribution to the area under the σ_1 curve in the FIR. Also shown is the scattering rate, Γ , which accounts for the broadening of the Drude-response due to scattering of the charge carriers. The results are representative for a significantly larger number of SLs that have been investigated. The value of ω_p^2 can be seen to decrease by more than an order of magnitude as the layer thickness is reduced from 60:60nm to 8:6nm. However, even the 8:6 nm SL, despite its very low ω_p^2 and the correspondingly low

density of the SC condensate, exhibits a superconducting transition in the measured resistivity at $T_c=60$ K. At the same time this SL still exhibits a ferromagnetic transition at $T_{mag}=120$ K. A significant suppression of ω_p^2 is evident already for the 16:16nm SL. This effect is most pronounced at 300 K, i.e. above the CMR transition at $T_{mag}=215$ K where the LCMO layers are known to remain insulating. The apparent increase in conductivity below 200 K is coincident with the FM transition and thus with the well known MIT transition in the LCMO layers that is at the heart of the CMR effect. This finding suggests that the metallicity of the YBCO layers is already almost entirely suppressed for the 16:16nm SL whereas the LCMO layers still become metallic below the FM transition. To confirm this interpretation, we fitted the response of the 16:16nm SL using the response functions of pure YBCO and LCMO layers (as measured by ellipsometry), as well as a theoretical fit function with a Drude plus a broad Lorentzian term to account for the so-called mid-infrared band. As shown in Fig. 2(e) we obtained a good fit at all temperatures for a model where the SL is composed of 16 nm LCMO and 16 nm of a fit layer with $\omega_p^2 = 0.03$ eV² (as in the 8nm:6nm SL). We were not able to fit the data with a model SL of 16 nm YBCO and 16nm fit layer.

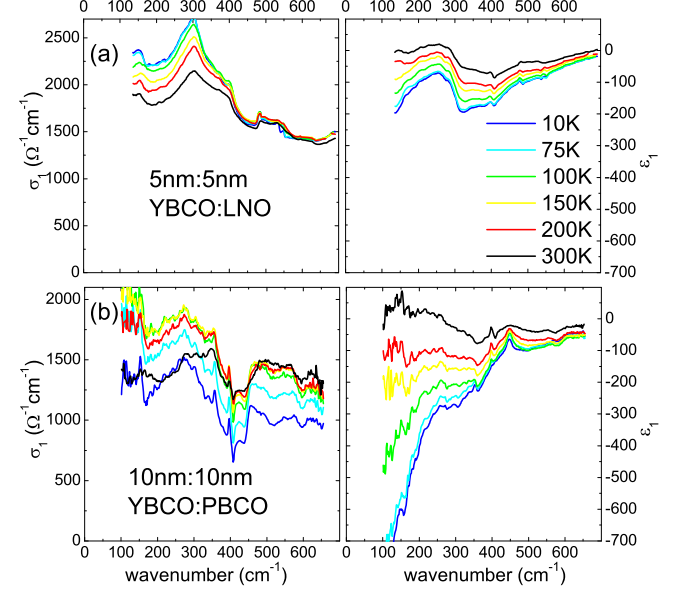
A corresponding suppression of metallicity is not observed for a SL where the FM metallic LCMO layers are replaced by layers of insulating $\text{PrBa}_2\text{Cu}_3\text{O}_7$ or LaNiO_3 (LNO), a paramagnetic metal (PM) that is character-

FIG. 2: in-plane conductivity, σ_1 , and the dielectric function, ϵ_1 for representative SLs with double layers of (a) 60nm:60nm, (b) 16nm:16nm, (c) 8nm:6nm, and (d) 5nm:5nm. (d) Numerical simulation for a SL with bilayers of 16nm normal LCMO and 16 nm fit layer with $\omega_p^2=0.03 \text{ eV}^2$ [similar to (c) and (d)]



ized by a broad Drude-peak and a strong electronic mode around 300 cm^{-1} ¹¹⁸. Figure 3(a) displays our ellipsometric data on a 5:5 nm SL of YBCO/LNO. It is immediately evident that this sample (despite of its very thin individual layers) maintains a metallic response with ω_p^2

FIG. 3: in-plane conductivity, σ_1 , and the dielectric function, ϵ_1 for representative SLs with double layers of (a) [5nm YBCO:5nm LNO]x20 and (b) [10nm YBCO:10nm PBCO]x20.



$= 1-1.2 \text{ eV}^2$. The apparent broadening of the Drude-response of this SL with $\Gamma \approx 70 \text{ meV}$ is partly due to the broad nature of the Drude response in LNO, but may also be caused by the waviness of the very thin layers or possibly also by the diffusion of a minor amount of Ni from the LNO to the YBCO layer. This effect may also be responsible for the sizeable suppression of T_c . Figure 3(b) shows that a similar persistence of metallicity is evident for a SL with 10:10 nm of $\text{YBa}_2\text{Cu}_3\text{O}_7/\text{PrBa}_2\text{Cu}_3\text{O}_7$ (YBCO/PBCO). Since it is well known that the PBCO layers are in an insulating state, it is clear that the free carrier response arises solely due to the metallic YBCO layers here.

Even for the YBCO/LCMO SLs we find that the metallic response can be recovered by changing the thickness ratio in favor of the YBCO layers. Figure 4 shows optical spectra on representative YBCO/LCMO SLs with a thickness ratio close to 3:1, for (a) 60:15nm, (b) 30:15nm, (c) 13:5nm and (d) 8:3nm. It is immediately evident that the 3:1 SLs exhibit a much weaker suppression of ω_p^2 than the 1:1 SLs shown in Fig. 2. Most instructive is the large difference between the 8:3nm and the 8:6nm SLs in Fig. 2(c) and 3(b). While the 8:6nm SL exhibits nearly insulating behavior, the signature of a sizeable free carriers response is clearly evident for the 8:3 nm SL. Such a result excludes any kind of structural or chemical imperfections of the SLs, such as the roughness of the interfaces or some kind of diffusion of the cations of the LCMO layer across the interfaces as a possible origin for the suppression of metallicity in the YBCO layer. As mentioned above, a poor material quality or a significant chemical mixing across the layer boundaries

is furthermore excluded by our x-ray, TEM and also by preliminary secondary ion mass spectrometry (SIMS) experiments. Furthermore, these problems should be even more severe for the 5:5nm YBCO/LNO SL which remains metallic.

A possible explanation of the dramatic suppression of metallicity in the 1:1 SC/FM SLs would be a massive transfer of holes from the YBCO layers to the LCMO layers. Such a transfer of about 3×10^{21} holes/cm³ could severely deplete the YBCO layers and, according to the phase diagram of LCMO¹⁹, could drive the LCMO layers into a charge ordered state similar to the one observed for a Ca content of $x > 0.45$. If this is the case, the LCMO is acting somewhat like an n-type semiconductor by accepting holes; however, the implied phase change to a charge ordered state differentiates this from a classical p-n junction, in addition to the large charge density involved. At a first glance one might think that such a scenario is not very likely. According to the simple depletion layer model of semiconductor theory²⁰, the Poisson equation is solved approximately with a quadratic potential difference on both sides of the interface giving a total depletion layer $d = \sqrt{2\varepsilon\Delta\phi/(\pi Ne)}$. Here N is the volume density of free carriers (assumed to be equal on the two sides of the interface), $\Delta\phi$ is the potential difference between the bulk and interface, ε is the static dielectric constant of the depleted insulating material (consisting of the electronic and phononic contributions), and e is the electron charge. Given a difference in work functions of 1 eV, and assuming a fairly large value $\varepsilon=15$, one expects the depletion layer of about 1 nm thickness, i.e., 1 monolayer of YBCO. However, estimates using the Lindhard dielectric function²⁰ for an anisotropic degenerate fermi-gas, parameterized so as to be representative of the layered YBCO, predict thicker depleted regions with Friedel oscillations of the charge density along the c -axis. The charge redistribution might actually affect several monolayers of (otherwise optimally doped) copper-oxygen layers in YBCO. Note that the charge depletion in infinite SL's would be symmetric at both interfaces of the YBCO layers.

Another equally interesting possibility is motivated by our observation that a suppression of metallicity occurs only in case of the FM layers LCMO and SRO whereas it is absent for the paramagnetic metal LaNiO₃. This suggests that magnetic correlations play an important role in the observed metal/insulator transition, possibly due to a novel magnetic proximity effect where charge carriers that are strongly coupled to different and competitive kinds of magnetic correlations, i.e. FM ones in the LCMO as opposed to AF or more exotic ones in YBCO, become localized. The underlying idea would be that the charge carriers gain mobility by adjusting their spins to the corresponding magnetic background, i.e. to the Cu moments in YBCO and the Mn(t_{2g}) moments in LCMO. Such a scenario is already well established for the case of LCMO where it leads to the well known CMR effect. For YBCO, however, this is not the case. Nevertheless,

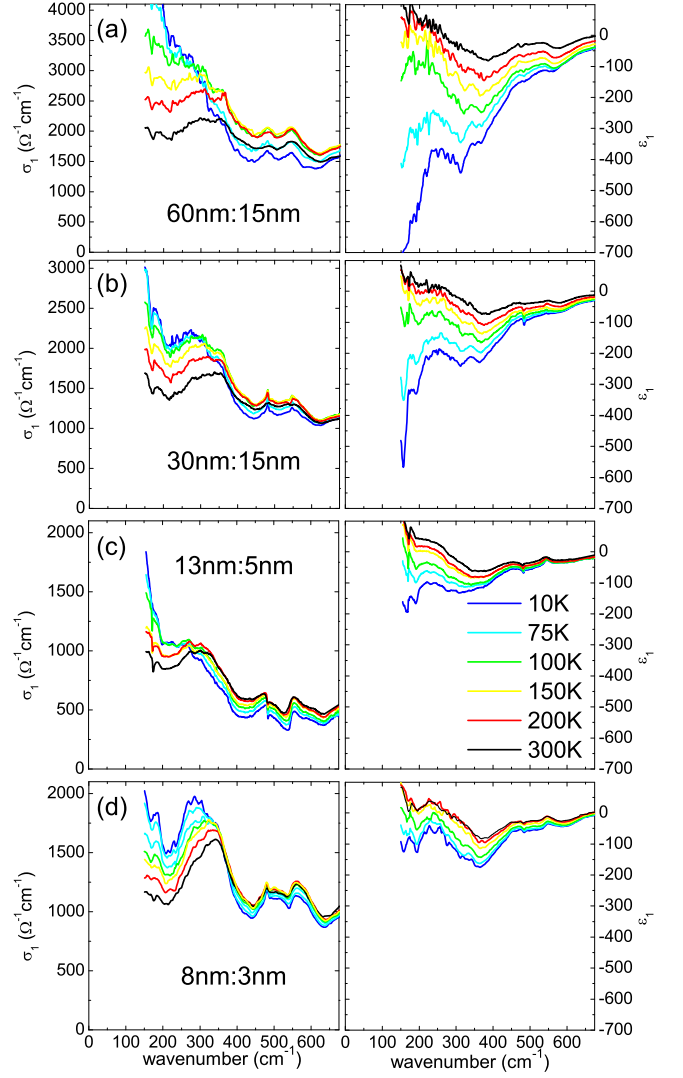


FIG. 4: in-plane conductivity, σ_1 , and the dielectric function, ε_1 for representative SLs with YBCO/LCMO ratios close to 3:1 (a) 60nm:15nm, (b) 30nm:15nm, (c) 13nm:5nm, and (d) 8nm:3nm.

it is known that AF correlations and fluctuations persist even for optimally doped samples. There exists clear evidence that the charge dynamics is strongly affected by the magnetic correlations, the most prominent example is the so-called pseudogap phenomenon in underdoped samples. Indeed, a number of models have been proposed where the mobility of the charge carriers strongly depends on the magnetic correlations and where a transition to a nearby insulating ground state can be induced by magnetic interactions, including the stripe phase^{21,22}, RVB-type²³, SO(5)²⁴, and the phase separation²⁵ models. The effect of a proximity coupling to a metallic FM layer has not been considered yet for any of these models.

In this context the most important aspect concerns the unexpectedly large length scale that is involved in the suppression of conductivity. There is indeed experi-

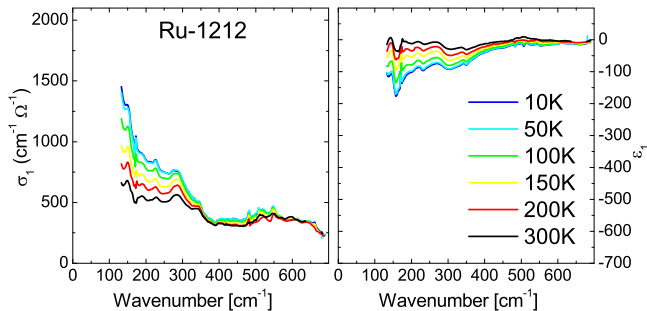


FIG. 5: in-plane conductivity, σ_1 , and the dielectric function, ϵ_1 for a laser ablation grown $\text{RuSr}_2\text{GdCu}_2\text{O}_8$ film.

mental indication that the spin coherence length in the cuprate HTSC is unusually large of the order of 20 nm^{26} or more²⁷. In addition, LCMO has a finite DOS near the Fermi level for both spin polarizations, although the spin mobility is much higher for the majority spins²⁸. Therefore it is not impossible that spin diffusion (driven by the gradient in spin polarization between LCMO and YBCO and opposed by the relaxation in the YBCO layer) may lead to a long-range spin polarization of the charge carriers deep inside the YBCO layers. Alternatively, the yet unknown novel magnetic ground state of the underdoped and optimal doped cuprate HTSC may be associated with an unusually large coherence length. Evidence for a long-range proximity effect has indeed been recently obtained in photo-doped $\text{YBa}_2\text{Cu}_3\text{O}_6$ ²⁹, where Josephson-tunneling currents were observed across undoped (AF) regions as wide as 100 nm .

Clearly, further experiments are required before one can distinguish between these equally fascinating possibilities. Most important will be direct measurements of the hole content within the CuO_2 planes which can be performed for example with the technique of core-level spectroscopy. Further attempts should include studies of the field-effect or of photo-induced conductivity as well as optical measurements in applied magnetic fields.

Finally, we make a comment on the infra-red conductivity of the hybrid ruthenate-cuprate compound $\text{RuSr}_2\text{GdCu}_2\text{O}_8$ (Ru-1212), in which SC within the CuO_2 layers ($T_c=50 \text{ K}$) and strong magnetism (with a sizeable FM component) in the RuO layers ($T_{mag}=135 \text{ K}$) can coexist within a unit cell³⁰. Thus in some sense it is a cuprate/magnetic SL, similar to these YBCO/LCMO SLs, with layer thicknesses of only a few angstrom. It is still debated whether the interaction between the SC and the magnetic order parameters is weak (this may be possible due to the layered structure), or whether their coupling is strong and therefore gives rise to a novel ground state with interesting new properties. Indeed some experiments indicate that the same charge carriers, which eventually become SC below T_c , are strongly coupled to the Ru magnetic moments^{31,32}. Another unusual feature of Ru-1212 is that it is a surprisingly poor conductor with

a low dc conductivity and extremely small SC condensate density as compared to other HTSCs³³. Figure 5 shows the infrared conductivity and dielectric function of a laser ablation grown Ru-1212 thin film. Raman and x-ray characterization of this film show it to be $\approx 95\%$ phase pure with the c-axis along the growth direction. Based on SQUID magnetization measurements the magnetic ordering transition of the Ru-moments occurs at $T_{mag}=145 \text{ K}$ and there is no evidence for superconductivity in this particular film. In fact it is commonly found for Ru-1212 that bulk superconductivity occurs only in samples with $T_{mag} \leq 135 \text{ K}$. Evidently, the free carrier response of this film with $\omega_p^2 \leq 0.3 \text{ eV}^2$ is much weaker than that of YBCO. The analogy to our artificial YBCO/LCMO SLs is rather striking and suggests that a related effect may be at work in the compound, which can be viewed as an intrinsic SL of a superconducting and magnetic layers.

IV. SUMMARY AND CONCLUSIONS

In conclusion, we have reported ellipsometric measurements of the far-infrared (FIR) dielectric properties of super-lattices (SLs) composed of thin layers of $\text{YBa}_2\text{Cu}_3\text{O}_7$ (YBCO) and $\text{La}_{0.67}\text{Ca}_{0.33}\text{MnO}_3$ (LCMO) that have been grown by laser ablation. Our optical data provide clear evidence that the free carrier response is strongly suppressed in these SLs as compared to the one in the pure YBCO and LCMO films. The suppression occurs in the normal as well as in the SC state and it involves a surprisingly large length scale of the order of $d_{\text{YBCO}}^{\text{crit}}=20 \text{ nm}$ and $d_{\text{LCMO}}^{\text{crit}}=10 \text{ nm}$. A similar suppression is observed for YBCO/ SrRuO_3 SLs. In stark contrast, a corresponding suppression of free carrier response does not occur for SLs where the FM LCMO is replaced by the paramagnetic metal LaNiO_3 . Possible explanations have been discussed in terms of a charge transfer between adjacent layers as well as charge localization due to magnetic correlations that are induced by a novel kind of long-range proximity effect. The low free carrier response observed in the far-infrared dielectric response of the magnetic superconductor $\text{RuSr}_2\text{GdCu}_2\text{O}_8$ is possibly related to this effect.

Acknowledgments

T.H. gratefully acknowledges the support of the Alexander von Humboldt Foundation. For technical help at the NSLS we thank L.G. Carr and C.C. Homes. The technical support by R.K. Kremer, E. Brücher, A. Stärke at MPI-FKF is highly appreciated. Some ellipsometry measurements have been performed by Julia Greisl from California Technical Institute during her stay at MPI-FKF.

-
- * Electronic address: tholden@brooklyn.cuny.edu
- ¹ for a review see L.N. Bulaevski et al., *Adv. Phys.* **34**, 175 (1985).
 - ² for a recent review see S.A. Wolf, D. D. Awschalom, R. A. Buhrman, J. M. Daughton, S. von Molnár, M. L. Roukes, A. Y. Chtchelkanova, and D. M. Treger, *Science* **294**, 1488 (2001).
 - ³ S. Saxena, P. Agarwal, K. Ahilan, F. M. Grosche, R. K. W. Haselwimmer, M. J. Steiner, E. Pugh, I. R. Walker, S. R. Julian, P. Monthoux, et al., *Nature* **406**, 587 (2001).
 - ⁴ S. Saxena and P. B. Littlewood, *Nature* **412**, 290 (2001).
 - ⁵ I. Bozovic, *IEEE T. Appl. Supercon.* **11**, 2686 (2001).
 - ⁶ H.-U. Habermeier, G. Cristiani, R. K. Kremer, O. Lebedev, and G. van Tendeloo, *Physica C* **364-365**, 298 (2001).
 - ⁷ L. Fàbrega, R. Rub, V. Vrtk, C. Ferrater, F. Sánchez, M. Varela, and J. Fontcuberta, *J. Magn. Mater.* **211**, 180 (2000).
 - ⁸ H. C. Yang, J. Chen, L. Wang, H. Sung, H. Horng, S. Yang, and J. Jeng, *J. Phys. Chem. Solid* **62**, 1837 (2001).
 - ⁹ G. Jakob, V. Moshchalkov, and Y. Bruynseraede, *Appl. Phys. Lett.* **66**, 2564 (1995).
 - ¹⁰ P. Prieto, P. Vivas, G. Campillo, E. Baca, L. F. Castro, M. Varela, C. Ballesteros, J. E. Villegas, D. Arias, C. León, et al., *J. Appl. Phys.* **89**, 8026 (2001).
 - ¹¹ P. Przyslupski, S. Kolesnik, E. Dynowska, T. Skoskiewicz, and M. Sawicki, *IEEE T. Appl. Supercon.* **7**, 2192 (1997).
 - ¹² A. Vigliante, U. Gebhardt, A. Rühm, P. Wochner, F. S. Razavi, and H.-U. Habermeier, *Europhys. Lett.* **54**, 619 (2001).
 - ¹³ R. Henn, C. Bernhard, A. Wittlin, M. Cardona, and S. Uchida, *Thin Solid Films* **313-314**, 643 (1998).
 - ¹⁴ A. Golnik, C. Bernhard, J. Humlíček, M. Kläser, and M. Cardona, *Phys. Stat. Sol. (b)* **215**, 553 (1999).
 - ¹⁵ J. Kircher, R. Henn, M. Cardona, P. L. Richards, and G. P. Williams, *J. Opt. Soc. Am. B* **14**, 705 (1997).
 - ¹⁶ K. Kamarás, K.-L. Barth, F. Keilmann, R. Henn, M. Reedyk, C. Thomsen, M. Cardona, J. Kircher, P. L. Richards, and J.-L. Stehlé, *J. Appl. Phys.* **78**, 1235 (1995).
 - ¹⁷ D. E. Aspnes, *Am. J. Phys.* **50**, 704 (1982).
 - ¹⁸ N. E. Massa, H. Falcón, H. Salva, and R. E. Carbonio, *Phys. Rev. B* **56**, 10178 (1997).
 - ¹⁹ P. Schiffer, A. P. Ramirez, W. Bao, and S.-W. Cheong, *Phys. Rev. Lett.* **75**, 3336 (1995).
 - ²⁰ N. W. Ashcroft and N. D. Mermin, *Solid State Physics* (Saunders College, Philadelphia, 1976).
 - ²¹ E. Demler, A. J. Berlinsky, C. Kallin, G. B. Arnold, and M. R. Beasley, *Phys. Rev. Lett.* **80**, 2917 (1998).
 - ²² V. Emery, S. A. Kivelson, and O. Zachar, *Phys. Rev. B* **56**, 6120 (1997).
 - ²³ P. W. Anderson, *Theory of Superconductivity in High T_c Cuprates* (Princeton University Press, Princeton, 1997).
 - ²⁴ S.-C. Zhang, *Science* **275**, 1089 (1997).
 - ²⁵ J. Burgy, M. Mayr, V. Martin-Mayor, A. Moreo, and E. Dagotto, *Phys. Rev. Lett.* **87**, 277202 (2001).
 - ²⁶ J. Y. T. Wei, *J. Superconduct.* **15**, 67 (2002).
 - ²⁷ S. P. Pai et al., cond-mat/0109388 (2001).
 - ²⁸ B. Nadgorny, I. I. Mazin, M. Osofsky, J. R. J. Soulen, P. Broussard, R. M. Stroud, D. J. Singh, V. G. Harris, A. Arsenov, and Y. Mukovskii, *Phys. Rev. B* **63**, 184433 (2001).
 - ²⁹ R. S. Decca, H. D. Drew, E. Osquiguil, B. Maiorov, and J. Guimpel, *Phys. Rev. Lett.* **85**, 3708 (2000).
 - ³⁰ C. Bernhard, J. L. Tallon, C. Niedermayer, T. Blasius, A. Golnik, E. Brücher, R. K. Kremer, D. R. Noakes, C. E. Stronach, and E. J. Ansaldo, *Phys. Rev. B* **59**, 14099 (1999).
 - ³¹ J. E. McCrone, J. Cooper, and J. Tallon, *J. Low Temp. Phys.* **117**, 1199 (1999).
 - ³² Y. Tokunaga, H. Kotegawa, K. Ishida, Y. Kitaoka, H. Takagiwa, and J. Akimitsu, *Phys. Rev. Lett.* **86**, 5767 (2001).
 - ³³ C. Bernhard, J. L. Tallon, E. Brücher, and R. K. Kremer, *Phys. Rev. B* **61**, 14960 (2000).